

NMR spectroscopy of 14-3-3 ζ reveals a flexible C-terminal extension: differentiation of the chaperone and phosphoserine-binding activities of 14-3-3 ζ

Danielle M. WILLIAMS*†, Heath ECROYD*‡, Katy L. GOODWIN*†, Huanqin DAI§, Haian FU||, Joanna M. WOODCOCK†, Lixin ZHANG§¹ and John A. CARVER*¹

*School of Chemistry and Physics, The University of Adelaide, Adelaide, SA 5005, Australia, †Centre for Cancer Biology, SA Pathology, Adelaide, SA 5000, Australia, ‡School of Biological Sciences, University of Wollongong, NSW 2522, Australia, §Chinese Academy of Sciences Key Laboratory of Pathogenic Microbiology and Immunology, Institute of Microbiology, Chinese Academy of Sciences, Beijing 100190, China, and ||Department of Pharmacology and Emory Chemical Biology Discovery Center, Emory University, Atlanta, GA 30322, U.S.A.

Intracellular 14-3-3 proteins bind to many proteins, via a specific phosphoserine motif, regulating diverse cellular tasks including cell signalling and disease progression. The 14-3-3 ζ isoform is a molecular chaperone, preventing the stress-induced aggregation of target proteins in a manner comparable with that of the unrelated sHsps (small heat-shock proteins). ¹H-NMR spectroscopy revealed the presence of a flexible and unstructured C-terminal extension, 12 amino acids in length, which protrudes from the domain core of 14-3-3 ζ and is similar in structure and length to the C-terminal extension of mammalian sHsps. The extension stabilizes 14-3-3 ζ , but has no direct role in chaperone action. Lys⁴⁹ is an important functional residue within the ligand-binding groove of 14-3-3 ζ with K49E 14-3-3 ζ exhibiting markedly reduced binding

to phosphorylated and non-phosphorylated ligands. The R18 peptide binds to the binding groove of 14-3-3 ζ with high affinity and also reduces the interaction of 14-3-3 ζ ligands. However, neither the K49E mutation nor the presence of the R18 peptide affected the chaperone activity of 14-3-3 ζ , implying that the C-terminal extension and binding groove of 14-3-3 ζ do not mediate interaction with target proteins during chaperone action. Other region(s) in 14-3-3 ζ are most likely to be involved, i.e. the protein's chaperone and phosphoserine-binding activities are functionally and structurally separated.

Key words: biophysical characterization, C-terminal flexibility, molecular chaperone, 14-3-3 protein, protein aggregation, protein–protein interaction.

INTRODUCTION

In mammals, the 14-3-3 family of ~30 kDa acidic proteins consists of seven isoforms (β , γ , ϵ , ζ , η , σ and τ) which are widely expressed in all tissues and organs. For example, they account for ~1% of the total soluble brain protein [1–3]. The different 14-3-3 isoforms form homo- and hetero-dimers that possess enhanced affinity to ligands containing phosphorylated serine or threonine residues within a specific sequence motif [4,5]. To date, more than 200 target proteins have been identified for 14-3-3 [6]. Depending on the nature of its target protein, the binding to 14-3-3 affects multiple signalling pathways which determine cell fate and organ development. For example, 14-3-3 association controls Raf signalling fidelity, neutralizes Bad-mediated apoptosis, and couples histone H3 with H4 to create a histone code for transcriptional elongation [2,3,7,8]. Through these highly regulated interactions, 14-3-3 proteins govern diverse physiological processes and cellular status. Furthermore, 14-3-3 proteins have been implicated in numerous disease states, including cancers and neurodegenerative diseases such as Alzheimer's disease, Parkinson's disease and ataxia. Various 14-3-3 isoforms are found to be associated with the intracellular deposits that are characteristic of Parkinson's disease and Alzheimer's disease. Furthermore, α -synuclein, the principal component of Lewy body deposits in Parkinson's disease, interacts with 14-3-3 and, because of this, both proteins have been implicated in the pathology of Parkinson's disease [1–3]. In the

same vein, 14-3-3 proteins have been implicated in Huntington's disease via interaction with the polyglutamine-containing protein huntingtin [9,10].

X-ray crystallographic studies have shown that each 14-3-3 monomer consists of a bundle of nine α -helices organized in an antiparallel fashion, forming a central amphipathic binding groove which is highly conserved across the 14-3-3 isoforms. The hydrophobic surface of this groove is formed from helices 7 and 9, with the opposing polar face consisting of basic and polar side chains of helices 3 and 5 (Figure 1A). The homo- and hetero-dimerization of 14-3-3 isomers occurs through N-terminal interactions of the monomers resulting in the two amphipathic grooves in each dimer combining to generate a 40 Å (1 Å = 0.1 nm) wide central channel [11] (Figure 1A). In the case of the 14-3-3 ζ isoform, the majority of its ligands interact with the binding groove via a conserved basic cluster (Lys⁴⁹, Arg⁵⁶ and Arg¹²⁷). Other residues along the polar and hydrophobic faces of the groove stabilize the ligand [3].

While amino acid sequences throughout the seven human 14-3-3 isoforms are generally highly conserved, particularly within the amphipathic binding groove, maximum sequence diversity is found in their extreme C-termini (encompassing, on average, the last 18 amino acids). Despite this diversity, the C-termini of all 14-3-3 isoforms share the characteristics of being acidic and contain a large number of amino acid residues which are disorder-promoting (Figure 1B, top panel). It has been proposed that the C-terminus of 14-3-3 ζ (Asp²³¹–Asn²⁴⁵) adopts a poorly

Abbreviations used: ADH, alcohol dehydrogenase; DLS, dynamic light scattering; DTT, dithiothreitol; α -LA, α -lactalbumin; MALLS, multi-angle laser light scattering; Ni-NTA, Ni²⁺-nitrilotriacetate; PDI, polydispersity index; ROESY, rotating-frame Overhauser enhancement spectroscopy; SEC, size-exclusion chromatography; sHsp, small heat-shock protein; TOCSY, total correlation spectroscopy; WT, wild-type.

¹ Correspondence may be addressed to either of these authors (email lzhang03@gmail.com or john.carver@adelaide.edu.au).

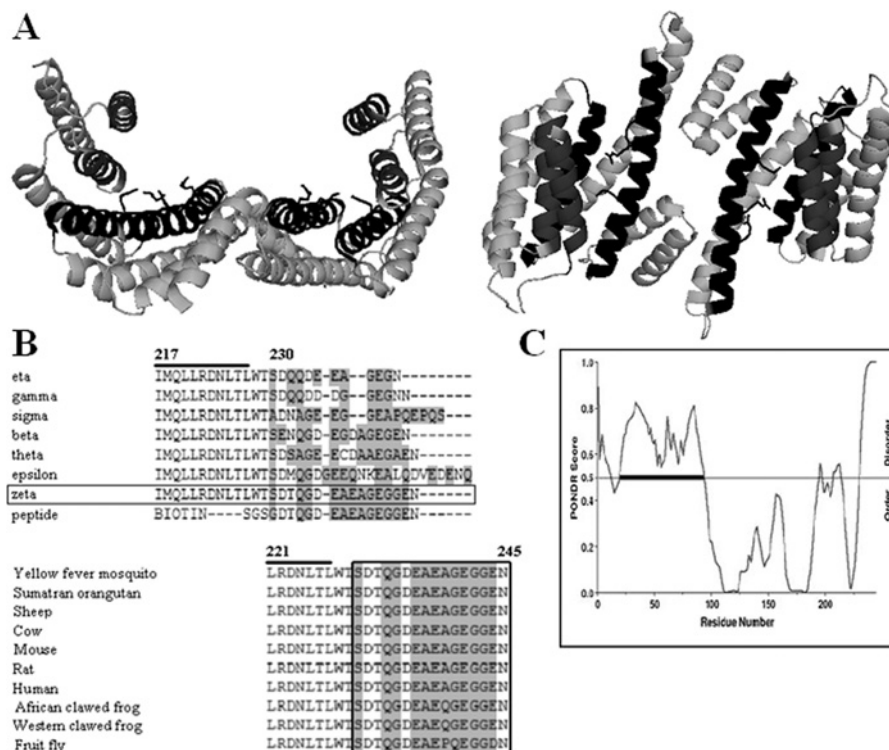


Figure 1 Structure of the 14-3-3 ζ dimer and ClustalW2 alignments of 14-3-3 C-termini with *in silico* predictions of their intrinsically disordered and ordered regions based on their primary amino acid sequences

(A) Front (left-hand panel) and top (right-hand panel) view of 14-3-3 ζ illustrating the dimeric structure of 14-3-3 proteins (PDB code: 1A38 [57]), viewed using PyMOL (<http://www.pymol.org>). Each monomer consists of nine α -helices, arranged in an antiparallel fashion. The amphipathic binding groove, composed of a hydrophobic side and polar side, is indicated in black. The side chains of Lys⁴⁹, Arg⁵⁶, Arg⁶⁰ and Arg¹²⁷ form a basic cluster at the bottom of the amphipathic binding groove. (B) ClustalW2 [26] alignments of 14-3-3 C-termini with disorder-promoting amino acids shaded grey. Top panel: comparison of the amino acid sequences of the synthesized peptide used in the present study (peptide) and the seven human 14-3-3 isoforms (η , γ , σ , β , θ , ϵ and ζ) aligned from the ninth α -helix (overline). The amino acid sequence of 14-3-3 ζ is boxed. Bottom panel: comparison of the C-terminal sequences of 14-3-3 ζ from a range of evolutionarily diverse species highlighting the high degree of sequence conservation and the inherent disorder within this region (boxed). (C) PONDR score [27–29] of 14-3-3 ζ where ordered and disordered regions of the protein are signified by a score of less than or more than 0.5 respectively. The thick black line on the 0.5 line indicates that this region was resolved in the crystal structure of the protein despite it being predicted to be disordered.

ordered conformation, the end of which is located near a basic cluster formed by the three arginine residues, Arg⁵⁶ and Arg⁶⁰ of helix 3, and Arg¹²⁷ of helix 5, which are all located within the polar face of the amphipathic binding groove [11]. Binding of the C-terminus to this basic cluster is proposed to result in occlusion of the binding groove and hence regulation of ligand binding [11–14]. In the crystal structures of 14-3-3 proteins, the C-terminal region is not resolved, implying that this region is conformationally mobile. In a significant development in 14-3-3 cellular function, the chaperone ability of 14-3-3 ζ has been described, whereby it prevents target proteins from amorously aggregating under conditions of stress [15]. In doing so, 14-3-3 ζ prevents the aggregation and precipitation of thermally aggregated target proteins in a manner akin to that of sHsps (small heat-shock proteins), a family of unrelated intracellular molecular chaperones. A common structural feature of mammalian sHsps is the marked intrinsic flexibility, polarity and unstructured nature of their extreme C-terminus, properties which are independent of the domain core of the oligomeric and heterogeneous protein [16–18]. The C-terminal extension in mammalian sHsps plays an important role in maintaining the solubility of the protein on its own and when it is in complex with aggregation-prone target proteins [19]. From the discussion above, 14-3-3 proteins may also have a flexible C-terminal extension which provides similar stability to it and the complex 14-3-3 ζ forms with target proteins.

The purpose of the present study was to understand further the structure and function of the C-terminus of 14-3-3 ζ and, in particular, its role in the chaperone action of 14-3-3 ζ . Accordingly, we have undertaken spectroscopic and biophysical characterization of the full-length protein and a truncated form from which the final 15 C-terminal amino acids were absent, i.e. Δ 15C 14-3-3 ζ . It is concluded that, like sHsps, 14-3-3 ζ has a short C-terminal extension that is flexible, polar and unstructured. Its function is to stabilize and solubilize the protein, and it has no direct role in its chaperone action. Furthermore, we investigated the role of the binding groove of 14-3-3 ζ in its chaperone action. It is concluded that the function of the binding groove for chaperone activity is not analogous to its role in phosphoserine peptide binding.

MATERIALS AND METHODS

Materials

All reagents used were of analytical grade and were obtained from Sigma–Aldrich unless otherwise specified. Unless otherwise stated, all solutions were prepared in 50 mM phosphate buffer containing, 100 mM sodium chloride and 0.05 % sodium azide, pH 7.4. Prior to use, all pre-existing aggregates were removed by filtration using a 0.22 μ M Minisart syringe filter (Sartorius). All protein concentrations were determined by their absorbance at

280 nm and calculated based on a subunit molecular mass. The R18 peptide was generated on an Applied Biosystem model 430A synthesizer by standard Merrifield solid-phase synthesis protocols and t-butoxycarbonyl chemistry.

Generation of Δ 15C 14-3-3 ζ constructs

The Δ 15C C-terminally truncated 14-3-3 ζ constructs were generated using the Stratagene QuikChange[®] site-directed mutagenesis kit following the manufacturer's protocol. The WT (wild-type) 14-3-3 ζ constructs in the pPRoEX vector were used as templates for mutagenesis to obtain Δ 15C-truncated plasmids that could be used in bacterial expression. The primers used for the PCR to exchange Asp²³¹ for a stop codon (underlined) were the 5'-GACATTGTGGA-CGTCGTAAAACCCAAGGAGACGAAG-3' oligonucleotide and its reverse complimentary strand. Successful mutagenesis was verified using DNA sequencing.

Expression and purification of WT and Δ 15C 14-3-3 ζ

Recombinant 14-3-3 ζ -His₆ fusion proteins were expressed under the control of the *trc* promoter in *Escherichia coli* BL21(DE3)-Codon Plus-RIL cells and subsequently purified using Ni-NTA (Ni²⁺-nitrilotriacetate) column chromatography (Qiagen). Following purification of the 14-3-3 ζ -His₆ fusion protein, cleavage of the His₆ tag was achieved using the tobacco etch virus protease, expressed under *tac* control in *E. coli* BL21(DE3)-Codon Plus-RIPL cells. After which, the cleavage products were purified using Ni-NTA column chromatography (Qiagen).

¹H-NMR spectroscopy

Peptide (biotin-SGSGDTQGDEAEAGEGGEN-OH) (Mimotopes) and protein samples (0.1 mM, 700 μ l) were prepared in 20 mM phosphate buffer, 10% ²H₂O/90% ¹H₂O and 0.05% sodium azide (pH 7.4) in 5 mm P-535 NMR tubes (Wilmad-Labglass, Quantum Scientific). All ¹H-NMR experiments were acquired at 600 MHz, with a sweep width of 7002 Hz at 25°C, using a Varian Inova-600 NMR spectrometer equipped with a pulsed-field gradient 5 mm probe. All spectral chemical shifts were referenced to the residual water resonance at 4.81 p.p.m. Through-bond (scalar) connectivities were obtained from TOCSY (total correlation spectroscopy) experiments with a spin-lock period of 60 ms [20]. Through-space connectivities were obtained for the peptide using ROESY (rotating-frame Overhauser enhancement spectroscopy) experiments with a mixing time of 100 ms [21]. All spectra were processed using VnmrJ (version 2.2d) software and visualized in Sparky 3 (<http://www.cgl.ucsf.edu/home/sparky/>).

Yeast two-hybrid analysis: galactosidase liquid assay

The strain EGY48 containing the pSH18-34 *lacZ* reporter plasmid (*MATa*, *trp1*, *his3*, *ura3*, *lexAops*-LEU2) of *Saccharomyces cerevisiae* was used for yeast two-hybrid interaction trap analysis. It was transformed with a bait plasmid encoding either the DNA-binding domain alone (vector), Raf-1, 14-3-3 ζ or a Bad-fusion protein. Both WT Bad and the S136A Bad mutant were used. A plasmid encoding either a 14-3-3 ζ WT or C-terminally truncated (Δ 15C) fusion protein was also co-transformed into these cells along with the *lacZ* reporter plasmid using the lithium acetate method [23]. Three individual colonies were randomly selected

for each experiment, and the assay was performed as described previously by Zhang et al. [23] and Truong et al. [14]. Cells were grown in glucose minimal medium and then transferred to galactose minimal medium to induce the expression of 14-3-3 ζ . The interaction between those fusion proteins reconstitutes a bipartite transcription factor that allows for the expression of β -galactosidase. The level of β -galactosidase activity thus indicates the amount of interaction between the two proteins. β -Galactosidase units were calculated by $D_{550}/(D_{550} \times \text{volume of cells} \times \text{time in minutes})$. The relative β -galactosidase units were estimated based on the following equation: β -galactosidase unit of test samples/ β -galactosidase unit of WT 14-3-3 ζ homodimers. Activities were obtained from at least three separate experiments, each performed in triplicate and results presented are means \pm S.D.

SEC (size-exclusion chromatography)-MALLS (multi-angle laser light scattering)

SEC-MALLS was performed using an S200HR 10/30 Superdex column (GE Healthcare) connected to a DAWN EOS multi-angle laser light-scattering detector (Wyatt Technology). Samples (100 μ l) were loaded on to the column at 10 mg/ml and eluted with 50 mM phosphate buffer containing 100 mM NaCl and 2 mM EDTA (pH 7.4) at a flow rate of 0.2 ml/min.

CD spectroscopy

The far-UV CD spectra of WT and truncated 14-3-3 ζ proteins (7.2 μ M, 200 μ l) were recorded on a Jasco J-815 spectropolarimeter over a wavelength range of 185–250 nm with a scan rate of 100 nm/min and a band-width of 1 nm. All data presented are the average of three accumulations obtained in 20 mM phosphate buffer (pH 7.4) and high-voltage tension records below 600 V. Protein thermostability CD profiles were recorded over a temperature range of 25–75°C at 5°C intervals. The temperature ramp rate was set at 2°C/min and once the desired temperature was reached, all solutions were equilibrated for 3 min prior to data collection.

DLS (dynamic light scattering)

For both WT and Δ 15C 14-3-3 ζ (7.2 μ M, 500 μ l), time-resolved DLS analysis was performed at 25°C and 37°C using a Zetasizer Nano-ZS (Malvern Instruments). Every 20 min (for up to 24 h), the particle diameter-intensity distribution and mean hydrodynamic diameter were determined from 13 acquired correlograms using the program CONTIN [24] and the method of cumulants [25] respectively, via the attached Dispersion Technology Software (Malvern Instruments).

Intrinsic tryptophan fluorescence

The tryptophan fluorescence of WT and Δ 15C 14-3-3 ζ (7.2 μ M, 2 ml) was measured using a Cary Eclipse fluorescence spectrophotometer equipped with a Peltier temperature controller (Varian). The temperature of the cell block was monitored between 37 and 80°C, and measurements were collected at 1°C intervals. For all recordings, the excitation wavelength was set to 295 nm, fluorescence emission was monitored between 300 and 400 nm, and the excitation and emission slit-widths were set to 5 nm.

Light scattering thermostability assays

The thermal stability of the 14-3-3 ζ proteins (7.2 μ M, 2 ml) in 50 mM phosphate buffer containing 100 mM NaCl and 2 mM EDTA (pH 7.4) was monitored by measuring the light scattering of the sample at 360 nm using a Cary 5000 UV-visible spectrophotometer equipped with a Peltier temperature controller (Varian). The absorbance of protein solutions was read at 1 °C intervals. The solutions were stirred for 1 min at each temperature prior to recording the light scattering. The time from temperature ramping to absorbance reading at each temperature was 2.5 min.

Urea denaturation

A stock solution of urea (8 M) was prepared volumetrically in 5 mM phosphate buffer (pH 7.4). Using a Hamilton Microlab apparatus (Taylor Scientific), the urea stock was systematically diluted into 5 mM phosphate buffer (pH 7.4) to produce 68 aliquots, each with a final volume of 800 μ l. A 100 μ l aliquot of 14-3-3 ζ was added to each 800 μ l aliquot to yield a final protein concentration of 2 μ M and a final urea concentration range of 0–7 M. The protein denaturation mixtures were equilibrated at room temperature (20 °C) for 3.5 h. The extent of unfolding for both WT and Δ 15C 14-3-3 ζ was assessed by acquiring the far-UV CD spectrum using a Jasco J-810 CD spectropolarimeter, and the signal was integrated between 215 and 230 nm. All data presented are the average of three accumulations and high-voltage tension records below 600 V.

Chaperone assays

α -LA (α -lactalbumin; 140 μ M), ADH (alcohol dehydrogenase; 14 μ M), insulin (44 μ M) and lysozyme (18 μ M), in a final volume of 200 μ l, were incubated in phosphate buffer (50 mM) containing NaCl (100 mM) and EDTA (2 mM) at 37 °C (pH 7.4), in the presence and absence of WT and Δ 15C 14-3-3 ζ (1:0–2 molar equivalents). In the case of α -LA, insulin and lysozyme, aggregation was initiated by the addition of DTT (dithiothreitol; final concentration 1 mM) just prior to incubation. Assays were conducted in 96-well plates (Interpath Services) with the aggregation and change in light scattering at 340 nm for each sample being measured and recorded in a Fluorostar Optima platereader (BMG Labtechnologies). Experiments containing K49E 14-3-3 ζ or the R18 peptide were carried out under the same conditions. When ADH was used as the target protein, the temperature was maintained at 42 °C. The chaperone assays with insulin in the presence of Mg²⁺ or spermine (at molar ratios of 0–50 and 0–2.0 respectively to 14-3-3 ζ) were conducted as described above, but with no EDTA present. In all cases, the quoted molar ratios refer to the moles of target protein monomer to moles of 14-3-3 ζ monomer.

RESULTS

The C-terminus of 14-3-3 ζ is highly conserved between species

14-3-3 proteins are a family of highly conserved proteins. However, as shown in Figure 1(B) (top panel), when the seven human 14-3-3 isoforms are aligned [26] there is little sequence similarity between them after the ninth α -helix. However, these last 14–25 amino acids share a high degree of disorder-promoting and acidic residues (e.g. glycine and glutamate in 14-3-3 ζ). When the C-terminal amino acids of 14-3-3 ζ are aligned across evolutionarily diverse species (Figure 1B, bottom panel) [26], there is a very high degree of sequence similarity, suggesting that this region plays an important role in the protein which has been conserved during evolution. Furthermore, based on its amino

acid sequence, the extreme C-terminus of 14-3-3 ζ is predicted by the PONDR [27–29] (Figure 1C) and FoldIndex [30] (results not shown) algorithms to be the most disordered region of the protein.

NMR identification of a flexible C-terminal extension in 14-3-3 ζ

Despite the relatively large mass of the 14-3-3 ζ dimer (~54 kDa), the one-dimensional ¹H-NMR spectrum of 14-3-3 ζ contains well-resolved relatively narrow resonances (results not shown), indicating that a portion(s) of the protein possesses inherent conformational mobility which is independent of the bulk of the 14-3-3 ζ dimer. To identify these flexible regions, a series of two-dimensional ¹H-¹H-NMR spectra were acquired for the full-length 14-3-3 ζ protein, a C-terminally truncated form of 14-3-3 ζ (Δ 15C) in which the last 15 C-terminal amino acids were absent, and a synthesized peptide (biotin-SGSGDTQGDEAEAGEGGEN-OH) corresponding to the last 15 C-terminal amino acids of 14-3-3 ζ with an additional four amino acids (SGSG) and a biotin moiety at its N-terminus. Figure 2(A) shows the N-H to α -CH, β -CH and γ -CH region of the TOCSY spectra for the C-terminal peptide (top panel) and full-length 14-3-3 ζ (bottom panel) obtained at 25 °C. Cross-peaks in these spectra arise from through-bond (scalar) connectivities. There is extensive coincidence of cross-peaks between the spectra of the C-terminal peptide and the full-length 14-3-3 ζ . By contrast, the C-terminal-deletion mutant did not give rise to well-resolved cross-peaks in the TOCSY spectrum (results not shown). Assignments of the cross-peaks arising from full-length 14-3-3 ζ and the C-terminal peptide were achieved from ROESY spectra via the sequential assignment procedure [31], in particular utilizing cross-peaks from the NH proton of residue $i + 1$ to the α -CH proton(s) of its preceding residue (i). Taken together these results indicated that the strongest cross-peaks in the two-dimensional NMR spectra of full-length 14-3-3 ζ were attributable to the 12 amino acid residues at the extreme C-terminus of the 14-3-3 ζ dimer (i.e. from Gly²³⁴ to Asn²⁴⁵), with no cross-peaks being observed for residues preceding Gly²³⁴. Also, when the α -CH chemical-shift values arising from full-length 14-3-3 ζ were compared with those of random coil values [32], no significant deviation was found (Figure 2B). The X-ray crystal structure of 14-3-3 ζ indicates that Trp²²⁸ is the first amino acid following the end of the ninth α -helix of 14-3-3 ζ [11]. From this, it can be inferred that the amino acids from Trp²²⁸ to Gln²³³ (inclusive) form a 'hinge' which has decreased conformational flexibility, spanning the region between the domain core of the protein and the 12 amino acids (Gly²³⁴–Asn²⁴⁵) at the extreme C-terminus of 14-3-3 ζ which have significantly enhanced flexibility.

The significant overlap of cross-peaks in the TOCSY spectra of 14-3-3 ζ from Gly²³⁴ to Asn²⁴⁵ with the peptide corresponding to the last 16 amino acids of the protein, the close similarity of α -CH chemical shifts to random coil values [32] and the presence of strong sequential NH _{$i+1$} to α -CH _{i} nuclear Overhauser effects show that the C-terminus of 14-3-3 ζ has an extended conformation with little or no preferred secondary structure, and a much greater degree of conformational flexibility than the rest of the protein. Thus 14-3-3 ζ has a flexible C-terminal extension encompassing its last 12 amino acids that is directly comparable with the C-terminal extension of mammalian sHsps in terms of its polar nature and conformational flexibility.

Role of the C-terminus in maintaining the gross conformation of 14-3-3 ζ

Since the C-terminal extension of sHsps plays an important role in the stability and function of the protein [16–19], an investigation

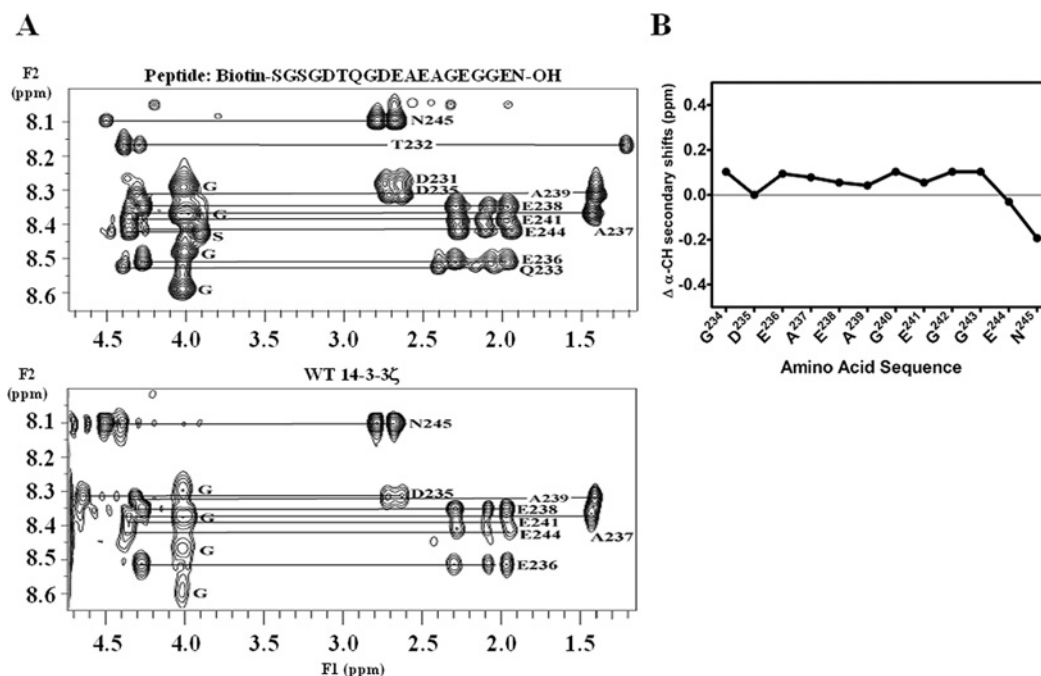


Figure 2 Two-dimensional ^1H - ^1H TOCSY NMR spectra of WT 14-3-3 ζ and a synthesized peptide corresponding to its C-terminus

(A) Two-dimensional ^1H - ^1H TOCSY spectrum at 25 °C of the NH to α -CH, β -CH, γ -CH region of the synthesized peptide corresponding to the C-terminus of 14-3-3 ζ (top panel) and WT 14-3-3 ζ (bottom panel). (B) The difference in α -CH ^1H chemical shifts of the C-terminal amino acids in 14-3-3 ζ from random coil values [32].

was undertaken to ascertain whether the C-terminal extension in 14-3-3 ζ has a similar role.

A yeast two-hybrid assay assessed the interaction *in vivo* of WT and Δ 15C 14-3-3 ζ with various ligands, i.e. WT 14-3-3 ζ and two proteins (Raf-1 and Bad) that are well-characterized ligands of 14-3-3 proteins [5] (Figure 3A). As expected, WT 14-3-3 ζ interacted well with itself to form a homodimer. Furthermore, WT 14-3-3 ζ formed a heterodimer with Δ 15C 14-3-3 ζ , and C-terminal truncation had no effect on the ability of 14-3-3 ζ to bind to either Raf-1 or Bad. Although the phosphorylation status of Bad at Ser¹³⁶ is a significant regulator of 14-3-3 ζ binding, there was some phosphorylation-independent binding to this ligand (i.e. to S136A Bad) by Δ 15C 14-3-3 ζ , which was not evident for WT 14-3-3 ζ . This slight difference may be due to the absence of the C-terminal extension in Δ 15C 14-3-3 ζ and is consistent with the proposed role of the extension in negatively regulating ligand binding to 14-3-3 ζ [11–14].

MALLS coupled with SEC, and DLS were used to determine whether truncation of 14-3-3 ζ affected its dimerization (Figures 3B and 3D). SEC–MALLS (Figure 3B) indicated that the average masses of WT (top panel) and Δ 15C (bottom panel) 14-3-3 ζ were 53.8 ± 5.9 kDa and 49.0 ± 0.5 kDa respectively, in good agreement with the predicted dimer masses (55.5 kDa and 52.6 kDa respectively). Each protein was also homogeneous, as indicated by their PDI (polydispersity index), which is quantified using the ratio between the molar mass of each protein averaged by weight (M_w) and number (M_n). The PDI (i.e. M_w/M_n) of WT and Δ 15C 14-3-3 ζ was 1.061 ± 0.127 and 1.003 ± 0.020 respectively.

Far-UV CD spectroscopy examined the effect of removing the C-terminal extension of 14-3-3 ζ on the overall secondary structure of the protein (Figure 3C). The CD spectrum of WT 14-3-3 ζ was comparable with that reported previously [23]. Truncation of 14-3-3 ζ resulted in a slight decrease in the mean residue ellipticity at 208 and 222 nm relative to the WT protein, implying reduced α -helical content for the truncated

mutant relative to the WT protein. As our NMR studies indicate that the C-terminal extension of 14-3-3 ζ adopts a disordered solvent-exposed structure in solution with no preferred secondary structure, the decreased CD minima observed for truncated 14-3-3 ζ relative to WT suggest that this extension stabilizes the domain core and α -helical content of the 14-3-3 ζ dimer.

DLS studies were undertaken to measure the hydrodynamic diameter and degree of heterogeneity of WT and Δ 15C 14-3-3 ζ in solution, as a means to determine whether truncation of 14-3-3 ζ affected its overall size and stability with time and temperature. As shown in Figure 3(D) (left-hand panel), the diameter of WT 14-3-3 ζ was stable over time, with a symmetrical distribution curve centred at 6.05 ± 0.50 nm at 25 °C. A very similar diameter was observed at 37 °C (6.27 ± 0.18 nm) which did not alter with time. The diameter of Δ 15C 14-3-3 ζ at 25 °C was not significantly different from that of the WT protein (7.21 ± 1.05 nm) and did not vary with time (Figure 3D, right-hand panel). However, at 37 °C, there was a time-dependency in the size of Δ 15C 14-3-3 ζ with its diameter increasing from 5.90 ± 1.22 nm to 14.18 ± 0.56 nm over 20 min of incubation, and then to 33.29 nm after 1360 min of incubation. Thus the truncated mutant has a tendency to aggregate at physiological temperature (Figure 3D, right-hand panel).

Thus, on the basis of the yeast two-hybrid studies, SEC, MALLS, CD and DLS analysis, it is concluded that although truncation of 14-3-3 ζ does not affect the ability of the protein to form dimers at 25 °C, the C-terminal extension is important in maintaining the overall shape, secondary structure and dimeric state of the protein at 37 °C.

Importance of the C-terminus in maintaining the thermo- and denaturant-stability of 14-3-3 ζ

The propensity of Δ 15C 14-3-3 ζ to thermal aggregation relative to WT 14-3-3 ζ , as indicated by DLS, led us to investigate

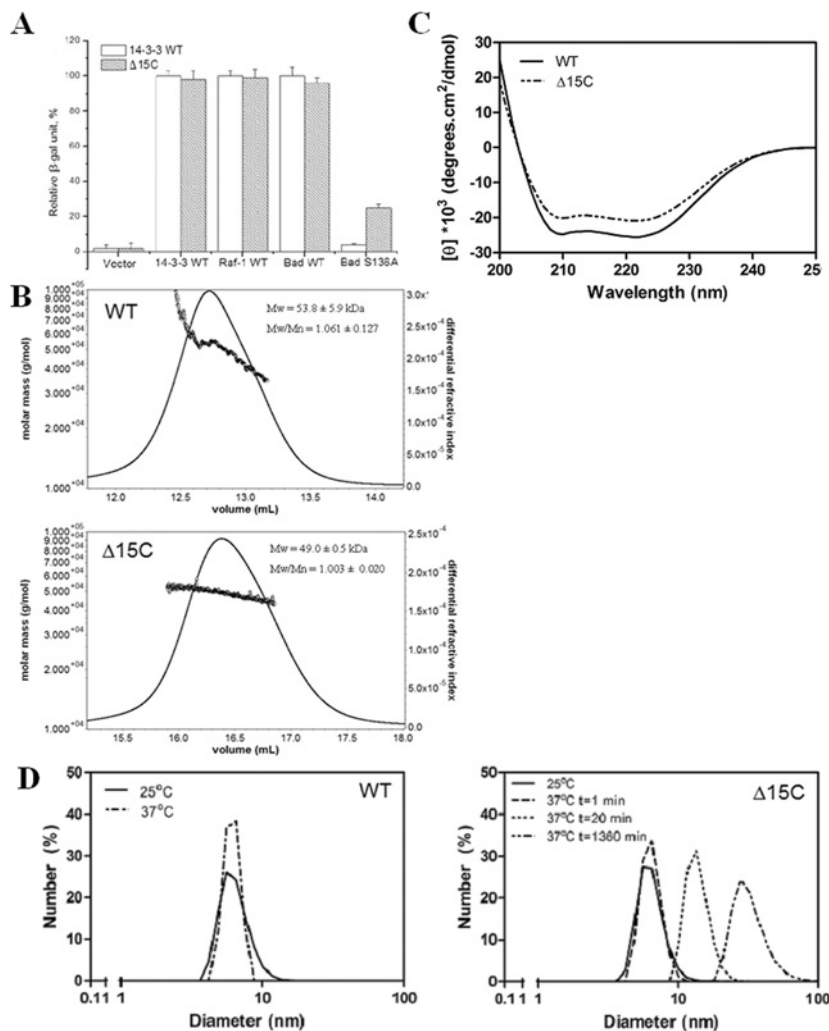


Figure 3 Yeast two-hybrid assays, SEC coupled with MALLS, far-UV CD spectra and DLS of WT 14-3-3 ζ and Δ 15C 14-3-3 ζ

(A) The ability of WT and Δ 15C 14-3-3 ζ to interact with the bait proteins Raf-1, Bad and S136A Bad in a yeast two-hybrid assay. Triplicate samples were used for this experiment and error bars indicate S.D. The results shown are representative of three individual experiments. (B) SEC coupled with MALLS illustrating the increase of Δ 15C 14-3-3 ζ 's elution volume and reduction in mass relative to WT 14-3-3 ζ . The continuous line represents UV absorption at 280 nm and circles represent the molecular mass of each protein obtained as a function of their elution volume. (C) The far-UV CD spectra of WT (continuous line) and Δ 15C (broken line) 14-3-3 ζ illustrating the decreased α -helical structure of the truncated protein at 37°C, as denoted by the decreased minima at 208 and 222 nm relative to that of WT 14-3-3 ζ . (D) DLS profiles of WT (left-hand panel) and Δ 15C (right-hand panel) 14-3-3 ζ at 25°C and 37°C, where the eluted particle size distribution is shown by number and demonstrates the propensity of Δ 15C 14-3-3 ζ to aggregate with time at 37°C.

the involvement of the C-terminal extension of 14-3-3 ζ in its thermostability in more detail. The alteration in structure of full-length and truncated 14-3-3 ζ as a function of temperature (37–80°C) was assessed by intrinsic fluorescence of the tryptophan residues (at positions 59 and 228). The wavelength of maximum tryptophan fluorescence emission (340 nm) was the same for both the WT and truncated protein and, over the temperature range tested, the emission profile did not undergo a red or blue shift for either protein (results not shown). Thus, over the temperature range examined, removal of the C-terminal extension of 14-3-3 ζ does not significantly alter the environment of the tryptophan residues within the protein.

The change in light scattering at 360 nm, as a function of temperature for WT and Δ 15C 14-3-3 ζ , was measured (Figure 4A). Initially both proteins were relatively stable displaying no significant alteration in light-scattering propensity between 37°C and 56°C. At 56°C, the Δ 15C 14-3-3 ζ solution underwent a marked increase in turbidity indicating significant aggregation of the protein. A second increase in turbidity occurred

at 74°C. The WT protein, on the other hand, displayed no change in light scattering until 60°C after which there was a slight increase. The precipitation profile for WT 14-3-3 ζ was also biphasic with a substantial increase in precipitation at 82°C.

The light-scattering data suggest that C-terminal truncation of 14-3-3 ζ decreases its thermostability and hence its C-terminal extension contributes to the stability of the protein. In agreement with this, the far-UV CD-melting profiles also indicated that the truncated protein had decreased thermostability relative to the WT protein, as quantified by a decrease in α -helical content of both proteins at 222 nm with increasing temperature due to unfolding and aggregation (Figure 4B). These data indicated that Δ 15C 14-3-3 ζ began to lose α -helical content at 32°C, whereas this did not occur until approximately 37°C for the WT protein. The melting points of the Δ 15C and WT proteins determined from the CD data were 56°C and 60°C respectively, and were directly comparable with the temperatures at which aggregation was observed by light scattering (Figure 4A). These data are also consistent with the DLS data in Figure 3(D) which highlight the

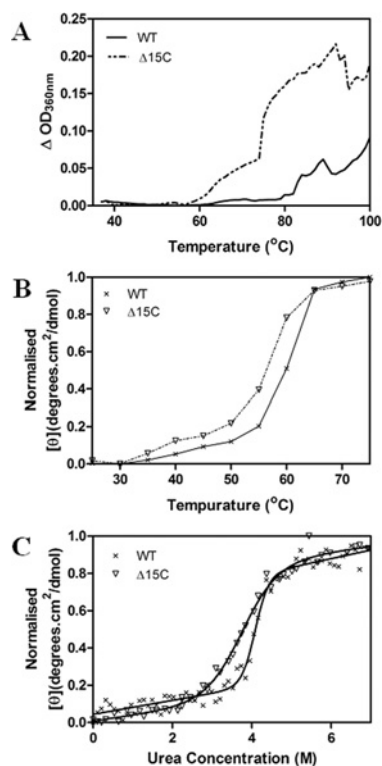


Figure 4 Light scattering and far-UV CD profiles of WT and $\Delta 15C$ 14-3-3 ζ proteins as a function of temperature or chemical denaturant

(A) The change in light scattering of WT (continuous line) and $\Delta 15C$ (broken line) 14-3-3 ζ at 360 nm as a function of temperature between 37 and 100 °C. (B) The change in molar ellipticity of WT (continuous line) and $\Delta 15C$ (broken line) 14-3-3 ζ at 222 nm as a function of temperature between 25 and 75 °C. The melting curve of $\Delta 15C$ relative to WT 14-3-3 ζ illustrates a decrease from 60 °C to 56 °C at which the mid-point of protein denaturation/unfolding occurs due to C-terminal truncation. (C) The integrated far-UV CD signal of WT (\times) and $\Delta 15C$ (∇) 14-3-3 ζ between 215 and 230 nm indicative of protein unfolding under denaturing conditions from 0 to 7 M urea. Curves are fitted to an equation describing the mid-point of denaturation. C-terminal truncation of 14-3-3 ζ reduces the half-point of unfolding by 0.33 M urea relative to the full-length protein.

greater tendency for $\Delta 15C$ 14-3-3 ζ to aggregate compared with the full-length protein.

Urea denaturation curves of WT and $\Delta 15C$ 14-3-3 ζ at 25 °C gave half-points of unfolding at 4.08 ± 0.03 and 3.75 ± 0.07 M urea respectively (Figure 4C). Thus truncation of the C-terminal extension led to decreased stability of 14-3-3 ζ to denaturant. It is therefore concluded that the C-terminal extension of 14-3-3 ζ has a role in maintaining the structural integrity of the domain core of the protein.

The effect of the C-terminal extension of 14-3-3 ζ on its chaperone ability

Previous studies by Yano et al. [15] showed that 14-3-3 ζ is capable of preventing the amorphous aggregation of citrate synthase induced by mild heat stress at 45 °C, and thus 14-3-3 ζ has chaperone activity. We confirmed this finding (results not shown) and extended it further by testing whether 14-3-3 ζ prevented amorphous target protein aggregation following chemical or reduction stress. We also investigated whether the C-terminus of 14-3-3 ζ was important for its chaperone activity. The amorphous aggregation of insulin can be induced by the addition of DTT, which reduces the intramolecular disulfide bonds, leading to the amorphous aggregation of the insulin

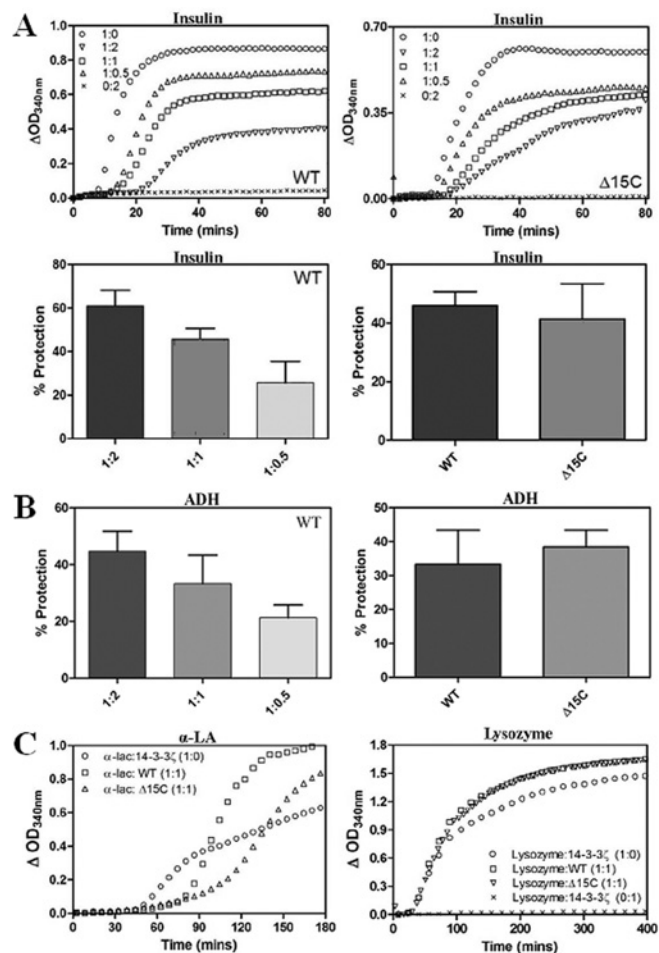


Figure 5 The chaperone ability of WT and $\Delta 15C$ 14-3-3 ζ against the amorphous aggregation of target proteins

(A) Top panels: the DTT-induced precipitation of insulin (44 μ M) in the presence of WT (left-hand panel) and $\Delta 15C$ (right-hand panel) 14-3-3 ζ at 1.0:0.5–2.0 molar ratios of insulin/14-3-3 ζ . Bottom panels: the percentage protection achieved by WT 14-3-3 ζ against the amorphous aggregation of reduced insulin at 1.0:0.5–2.0 molar ratios of insulin/WT (left-hand panel). A comparison of the chaperone ability of WT and $\Delta 15C$ 14-3-3 ζ against the aggregation of insulin using the percentage protection afforded at a 1:1 molar ratio of insulin/14-3-3 ζ (right-hand panel). (B) The percentage protection achieved by WT 14-3-3 ζ against the chemically induced aggregation of ADH (14 μ M) at 1.0:0.5–2.0 molar ratios of ADH/WT (left-hand panel). A comparison of the chaperone ability of WT and $\Delta 15C$ 14-3-3 ζ against the aggregation of ADH using the percentage protection afforded at a 1:1 molar ratio of ADH/14-3-3 ζ (right-hand panel). (C) DTT-induced precipitation of α -LA (140 μ M) in the absence (\circ) and presence of WT (\square) and $\Delta 15C$ (Δ) 14-3-3 ζ at 1:1 molar ratios of α -LA/14-3-3 ζ (left-hand panel). The DTT-induced precipitation of lysozyme (18 μ M) in the absence (\circ) and presence of WT (\square) and $\Delta 15C$ (∇) 14-3-3 ζ at 1:1 molar ratios of lysozyme/14-3-3 ζ (right-hand panel). For each target protein, the assay was conducted in triplicate, repeated a minimum of three times, and the data used to calculate the percentage protection afforded by either WT or $\Delta 15C$ 14-3-3 ζ . Results are presented as means \pm S.E.M. In all cases, the percentage protection was calculated once protein aggregation had reached a plateau.

B-chain. In the absence of 14-3-3 ζ , this resulted in an increase in light scattering 10 min after the addition of DTT. The light scattering due to the precipitation of insulin B-chain reached a maximum after 40 min. Both the truncated and full-length forms of 14-3-3 ζ suppressed the aggregation and precipitation of insulin in a concentration-dependent manner (Figure 5A, top panels). At a 1:1 molar ratio of insulin/WT 14-3-3 ζ , the precipitation of insulin was suppressed by 46 ± 5 % (Figure 5A, bottom left-hand panel). At this ratio, the truncated protein had similar chaperone-like activity (41 ± 12 %) in this assay (Figure 5A, bottom right-hand panel).

Similar results were also obtained when ADH was used as the target protein (Figure 5B). The amorphous aggregation of ADH can be induced by chelation of its Zn^{2+} ion using EDTA. In the absence of 14-3-3 ζ , precipitation of ADH commenced 60 min after incubation with EDTA, reaching a maximum after 300 min (results not shown). As seen for insulin, both full-length and truncated forms of 14-3-3 ζ suppressed the increase in light scattering associated with ADH precipitation in a concentration-dependent manner such that, at a 1:1 molar ratio of ADH/WT 14-3-3 ζ , aggregation was suppressed by $33 \pm 11\%$ (Figure 5B, left-hand panel). No significant differences were observed in the chaperone ability between the full-length and truncated protein in this assay (Figure 5B, right-hand panel). No high-molecular-mass complexes were observed by SEC of the soluble fraction at the completion of either of these amorphous aggregation assays, suggesting that the interaction between 14-3-3 ζ and its target proteins is transient (results not shown).

The chaperone ability of 14-3-3 ζ to inhibit the aggregation of reduced insulin was also tested in the presence of excess Mg^{2+} and the polyamine spermine (at 0–50 and 0–2.0 molar equivalents respectively). Both species interact electrostatically and strongly with the negatively charged C-terminal extension of 14-3-3 ζ [33]. Under both sets of conditions, there was no statistical difference between the chaperone ability of 14-3-3 ζ in the presence and absence of Mg^{2+} and spermine (results not shown). Thus these data are consistent with the lack of direct involvement of the C-terminal extension in the chaperone action of 14-3-3 ζ .

When reduced α -LA was used as the target protein, truncated and full-length 14-3-3 ζ were ineffective chaperones (Figure 5C, left-hand panel). In the absence of 14-3-3 ζ , α -LA aggregation induced by reduction caused an increase in light scattering at approximately 50 min which reached a plateau after 120 min. Truncated 14-3-3 ζ (at a 1:1 molar ratio to α -LA) increased the lag phase of α -LA aggregation to 104 ± 7 min, as compared with when the full-length protein was present, in which case the lag phase was 84 ± 3 min. However, both forms of 14-3-3 ζ caused enhanced precipitation (Figure 5C, left-hand panel). Analysis of the precipitates after completion of the experiment by SDS/PAGE revealed the presence of both 14-3-3 ζ and α -LA (results not shown), i.e. the chaperone action of 14-3-3 ζ with reduced α -LA led to complexation and co-precipitation. The chaperone ability of WT and $\Delta 15C$ 14-3-3 ζ was also tested against the DTT-induced aggregation of lysozyme, a protein that is structurally related to α -LA [34]. Interestingly, the light-scattering profile of reduced lysozyme was slightly enhanced by the presence of either WT or $\Delta 15C$ 14-3-3 ζ , i.e. neither protein prevented reduced lysozyme from aggregating and precipitating (Figure 5C, right-hand panel). After completion of this assay, analysis of the supernatants by analytical SEC showed a decrease in the amount of 14-3-3 ζ in solution when incubated in the presence of lysozyme (results not shown). Thus both WT and $\Delta 15C$ 14-3-3 ζ interact with reduced lysozyme in a manner similar to that with reduced α -LA, resulting in co-precipitation of both proteins from solution.

To gain insight into whether the amphipathic binding groove of 14-3-3 ζ is involved in chaperone action, the chaperone activity of K49E 14-3-3 ζ and of the WT protein in the presence of the R18 peptide was investigated. Charge reversal at Lys⁴⁹ (i.e. in K49E) gives rise to a protein that binds phosphorylated and non-phosphorylated ligands with significantly reduced affinity [23]. The R18 peptide binds to the amphipathic binding groove of 14-3-3 ζ with high affinity ($K_d = 80$ nM), preventing ligand interactions, e.g. with ExoS and Raf [35,36]. However, the K49E mutation and the presence of the R18 peptide did not affect the chaperone activity of 14-3-3 ζ (Figure 6). Therefore it is unlikely that the binding groove of 14-3-3 ζ , particularly its hydrophilic side, is

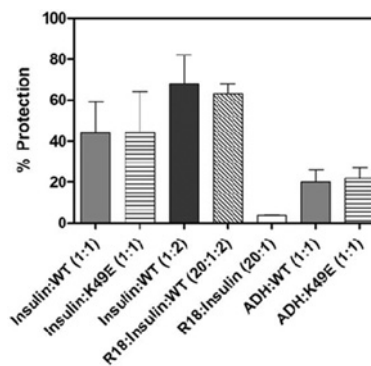


Figure 6 The chaperone ability of WT and K49E 14-3-3 ζ against the amorphous aggregation of insulin and ADH

The percentage protection afforded against the DTT-induced aggregation of insulin ($44 \mu M$) and chemically induced aggregation of ADH ($14 \mu M$) by WT and K49E 14-3-3 ζ at a 1:1 molar ratio of target protein/14-3-3 ζ . The percentage protection afforded against the DTT-induced aggregation of insulin ($44 \mu M$) by WT 14-3-3 ζ in the presence and absence of the R18 peptide at a 20:1:2 molar ratio of R18/insulin/WT 14-3-3 ζ . For each target protein, the assay was conducted in triplicate, repeated a minimum of three times and the data used to calculate the percentage protection afforded by either K49E 14-3-3 ζ or WT 14-3-3 ζ in the presence and absence of the R18 peptide. Results are presented as means \pm S.D. The percentage protection was calculated once protein aggregation had reached a plateau.

involved in the interaction with target proteins during chaperone action.

DISCUSSION

Consistent with folding prediction algorithms, the NMR data indicate that the last 12 C-terminal amino acids of 14-3-3 ζ (Gly²³⁴–Asp²⁴⁵) are solvent-exposed and exhibit flexibility that is independent of the domain core of the protein, while adopting no preferred secondary structure. This structural motif is akin to the C-terminal extension in mammalian sHsps (e.g. αA - and αB -crystallin) which is similar in length to that in 14-3-3 ζ and is also unstructured, flexible and highly dynamic in nature [17,18,37,38]. Indeed, the C-terminal extension in both proteins has characteristics that are comparable with those of an isolated peptide of the same sequence in solution [39]. Therefore it is concluded that 14-3-3 ζ , and by analogy all other 14-3-3 proteins, have a flexible C-terminal extension.

The inherent flexibility of the C-terminal extension of 14-3-3 ζ and its structural similarity to that of sHsps, along with its conservation across species, indicate that the C-terminal extension of 14-3-3 ζ may play an important role in the function and stability of the protein. Indeed, Silhan et al. [12], Obsilova et al. [13] and Truong et al. [14] proposed that, in the absence of a ligand, the C-terminus of 14-3-3 ζ utilizes its negative charges to occupy the peptide-binding groove of the protein and thereby regulates binding of ligands, particularly phosphorylated ones, to the binding groove. Our NMR results indicating that the C-terminal extension is flexible are not inconsistent with this proposal. The extension could interact transiently with the peptide-binding groove and give rise to the fluorescence responses between the two regions that are observed by Obsil and co-workers [12,13]. The much shorter timescale of the fluorescence compared with the NMR experiments is compatible with this proposal. Furthermore, the well-conserved ‘hinge’ region, Trp²²⁸–Gln²³³ (Figure 1B), which is not mobile enough to be observed by NMR spectroscopy but is not part of the last helix [11], may

occupy the binding groove principally via its negatively charged residue Asp²³¹.

Using an *in vivo* yeast two-hybrid assay and a range of *in vitro* spectroscopic and biophysical techniques, the structural and functional roles of the C-terminal extension was investigated by comparing the full-length protein with a C-terminally truncated form (Δ 15C 14-3-3 ζ). Truncation did not affect the ability of 14-3-3 ζ to form dimers *in vitro* or *in vivo*, or to dimerize with WT 14-3-3 ζ . In yeast two-hybrid assays, C-terminal truncation also had no effect on the ability of WT and Δ 15C 14-3-3 ζ to bind to the phosphorylated ligands Raf and Bad. However, although C-terminal truncation of 14-3-3 ζ did not significantly alter the average diameter of the dimer at 25 °C, at physiological temperature, the truncated protein aggregated progressively with time. C-terminal truncation also slightly decreased the α -helical content of 14-3-3 ζ . Thus the C-terminal extension of 14-3-3 ζ is important in maintaining the overall structural integrity of the protein without directly being involved in dimer formation. Consistent with this, C-terminal truncation resulted in a significant decrease in the thermostability of the protein, and enhanced its susceptibility to denaturant. Obsil and co-workers [12,13] also concluded that the C-terminal extension stabilizes 14-3-3 ζ in the absence of a binding ligand. Finally, similarly to 14-3-3 ζ , the C-terminal extension in mammalian sHsps also plays a vital role in the overall thermostability, solubility and structure of the protein and the large and heterogeneous complexes they form with target proteins during chaperone action [16,17,19,38].

The chaperone activity of the full-length and truncated 14-3-3 ζ proteins was investigated using a variety of target proteins undergoing amorphous aggregation induced by heat or reduction. In comparison with the sHsp α B-crystallin, 14-3-3 ζ was a 4-fold poorer chaperone in preventing the aggregation of reduced insulin [40,41]. In sHsps, truncation or site-specific mutations within the C-terminal extension result in an alteration in chaperone action [19,42–44]. In contrast, removal of this region in 14-3-3 ζ had little effect on its chaperone activity against the aggregating target proteins insulin and ADH. Likewise, binding of positively charged species (Mg²⁺ and spermine) to the C-terminal extension of 14-3-3 ζ did not affect its chaperone activity. With reduced α -LA, removal of the C-terminal extension of 14-3-3 ζ led to a delay in onset of aggregation of α -LA compared with the situation for WT 14-3-3 ζ . However, in both cases, co-precipitation of α -LA and 14-3-3 ζ occurred. With reduced lysozyme, the presence of WT and Δ 15C 14-3-3 ζ also increased the precipitation of both proteins at 37 °C, but to a smaller degree relative to that of α -LA, and with no alteration in the onset of aggregation. A naturally occurring mutant of α B-crystallin, R120G, is associated with desmin-related myopathy [45]. R120G α B-crystallin has a destabilized structure [46] and also causes enhanced precipitation of itself and reduced α -LA [46,47], which possibly arises from greater exposure of the chaperone-binding site(s) in R120G α B-crystallin compared with the WT protein. Similar behaviour may be occurring with 14-3-3 ζ whereby interaction with reduced α -LA leads to formation of the 14-3-3 ζ / α -LA complex which is not stable in solution due to greater exposed hydrophobicity.

Charge reversal mutants of the conserved basic residues on the polar side of the binding groove of 14-3-3 ζ , in particular K49E, result in a drastic reduction of 14-3-3 ζ ligand affinity presumably due to electrostatic repulsion, indicating that the conserved basic residues within the ligand-binding groove of 14-3-3 ζ are important for ligand interaction [23]. However, based on the very similar chaperone activity of K49E and WT 14-3-3 ζ , and the lack of effect of the R18 peptide, a species that has avid affinity for the binding groove, on the chaperone activity of 14-3-3 ζ , it seems unlikely that the amphipathic binding groove of

14-3-3 ζ (or at least its hydrophilic side) is a major determinant in chaperone action. The C-terminal extension of 14-3-3 ζ also appears to not be involved in the interaction with target proteins during chaperone action. Thus other region(s) may encompass the chaperone-binding site(s) of 14-3-3 ζ , possibly on the exterior of the protein. Examination of the crystal structure of 14-3-3 ζ [11] does not reveal any obvious regions of clustered hydrophobicity on its surface that may be potential chaperone-binding sites. Potentially, the hydrophobic side of the binding groove may be a factor in regulating chaperone activity, e.g. the conserved residues Leu¹⁷² and Leu²²⁰ in helices 7 and 9. Future studies will explore this possibility via site-directed mutagenesis.

No high-molecular-mass complexes were isolated between 14-3-3 ζ and its target proteins, suggesting an interaction which is transient in nature, similar to the interaction observed between mammalian sHsps and some target proteins under mild stress conditions [40,41]. Despite the similarity in mechanism between the interaction of target proteins with 14-3-3 ζ and sHsps, the C-terminal extension of 14-3-3 ζ is not required to maintain the solubility of the 14-3-3 ζ -target protein complex, nor does its removal affect chaperone activity. The difference in dependency between 14-3-3 ζ and sHsps on their C-terminal extension during chaperone action may be due to 14-3-3 ζ not undergoing subunit exchange as part of a large heterogeneous complex, as is the case for mammalian sHsps. For the latter, subunit exchange is linked to sHsp chaperone action [48] and may intimately involve the C-terminal extension [49]. The inability of 14-3-3 ζ to prevent the aggregation of the related reduced target proteins α -LA and lysozyme is indicative of the selective nature of the chaperone action of 14-3-3 ζ and the need to utilize a range of target proteins to explore its chaperone action. Variation in chaperone ability with target proteins is also observed with sHsps and is related to factors such as the rate of target protein aggregation, the nature of the intermediate state of the target protein, the mass of the target protein and the type of target protein aggregation [38,40,41,50–53]. Similar factors are most likely to be important in determining the efficiency of 14-3-3 ζ chaperone action.

Our understanding of the function of 14-3-3 proteins as molecular chaperones is in its infancy. It has previously been established that 14-3-3 ζ has a regulatory role in the formation of intracellular tau filaments [54,55] as occurs in Alzheimer's disease, and also in the aggregation of polyglutamine proteins, such as ataxin-1 and huntingtin [9,10,56]. In the case of tau, one mode of 14-3-3 ζ interaction is dependent on tau phosphorylation [54], implying that 14-3-3 ζ interacts with tau via its amphipathic binding groove. The present study and previous studies [15] demonstrate a different role for 14-3-3 ζ as a molecular chaperone in preventing the aggregation of partially folded target proteins. The results of the present study indicate that the amphipathic groove may not be required for this interaction. The implication is that 14-3-3 ζ has diverse roles in protein misfolding and aggregation and strengthens the notion of the involvement of 14-3-3 proteins in neurodegenerative diseases such as Alzheimer's disease, Parkinson's disease and Huntington's disease.

AUTHOR CONTRIBUTION

Danielle Williams designed and performed most of the experiments and, with John Carver, wrote the paper. John Carver also devised the overall experimental concepts and content of the paper. Huanqin Dai, Haian Fu, Lixin Zhang and Katy Goodwin conducted the remaining experiments and undertook a critical review of the manuscript. Heath Ecroyd and Joanna Woodcock provided assistance with, and design of, the experiments along with a critical review of the paper.

ACKNOWLEDGEMENTS

We acknowledge the technical support of Phil Clements (University of Adelaide), Dr Keith Shearwin (University of Adelaide) and Alexander Buell (University of Cambridge). The CD spectra were acquired at the Biophysical Characterisation Facility, Adelaide, Australia.

FUNDING

This work was supported, in part, by the China Important National Science and Technology Specific Projects [grant number 2008ZX09401-05 (to L.Z.)] and the Australian Research Council (to J.C.). L.Z. was an awardee of the Hundred Talents Program. H.E. was supported by an Australian National Health and Medical Research Council Peter Doherty Biomedical Fellowship. D.W. was the recipient of an Australian Postgraduate Award and was partially funded by the Daphne Elliott Bursary, AUGC/RC Heddlie Award, George Murray Scholarship and an Australian Bicentennial Scholarship.

REFERENCES

- Aitken, A. (2006) 14-3-3 proteins: a historic overview. *Semin. Cancer Biol.* **16**, 162–172
- Dougherty, M. K. and Morrison, D. K. (2004) Unlocking the code of 14-3-3. *J. Cell Sci.* **117**, 1875–1884
- Fu, H., Subramanian, R. R. and Masters, S. C. (2000) 14-3-3 proteins: structure, function, and regulation. *Annu. Rev. Pharmacol. Toxicol.* **40**, 617–647
- Muslin, A. J., Tanner, J. W., Allen, P. M. and Shaw, A. S. (1996) Interaction of 14-3-3 with signaling proteins is mediated by the recognition of phosphoserine. *Cell* **84**, 889–897
- Yaffe, M. B., Rittinger, K., Volinia, S., Caron, P. R., Aitken, A., Leffers, H., Gambin, S. J., Smerdon, S. J. and Cantley, L. C. (1997) The structural basis for 14-3-3:phosphopeptide binding specificity. *Cell* **91**, 961–971
- Rubio, M. P., Geraghty, K. M., Wong, B. H. C., Wood, N. T., Campbell, D. G., Morrice, N. and Mackintosh, C. (2004) 14-3-3 affinity purification of over 200 human phosphoproteins reveals new links to regulation of cellular metabolism, proliferation and trafficking. *Biochem. J.* **379**, 395–408
- Zhang, L., Chen, J. and Fu, H. (1999) Suppression of apoptosis signal-regulating kinase 1-induced cell death by 14-3-3 proteins. *Proc. Natl. Acad. Sci. U.S.A.* **96**, 8511–8515
- Zippo, A., Serafini, R., Rocchigiani, M., Pennacchini, S., Krepelova, A. and Oliviero, S. (2009) Histone crosstalk between H3S10ph and H4K16ac generates a histone code that mediates transcription elongation. *Cell* **138**, 1122–1136
- Waelter, S., Boeddrich, A., Lurz, R., Scherzinger, E., Lueder, G., Lehrach, H. and Wanker, E. E. (2001) Accumulation of mutant huntingtin fragments in aggresome-like inclusion bodies as a result of insufficient protein degradation. *Mol. Biol. Cell* **12**, 1393–407
- Omi, K., Hachiya, N. S., Tanaka, M., Tokunaga, K. and Kaneko, K. (2008) 14-3-3 ζ is indispensable for aggregate formation of polyglutamine-expanded huntingtin protein. *Neurosci. Lett.* **431**, 45–50
- Liu, D., Bienkowska, J., Petosa, C., Collier, R. J., Fu, H. and Liddington, R. (1995) Crystal structure of the ζ isoform of the 14-3-3 protein. *Nature* **376**, 191–194
- Silhan, J., Obsilova, V., Vecer, J., Herman, P., Sulc, M., Teisinger, J. and Obsil, T. (2004) 14-3-3 protein C-terminal stretch occupies ligand binding groove and is displaced by phosphopeptide binding. *J. Biol. Chem.* **279**, 49113–49119
- Obsilova, V., Herman, P., Vecer, J., Sulc, M., Teisinger, J. and Obsil, T. (2004) 14-3-3 ζ C-terminal stretch changes its conformation upon ligand binding and phosphorylation at Thr²³². *J. Biol. Chem.* **279**, 4531–4540
- Truong, A. B., Masters, S. C., Yang, H. and Fu, H. (2002) Role of the 14-3-3 C-terminal loop in ligand interaction. *Proteins* **49**, 321–325
- Yano, M., Nakamura, S., Wu, X., Okumura, Y. and Kido, H. (2006) A novel function of 14-3-3 protein: 14-3-3 ζ is a heat-shock-related molecular chaperone that dissolves thermal-aggregated proteins. *Mol. Biol. Cell* **17**, 4769–4779
- Carver, J. A. (1999) Probing the structure and interactions of crystallin proteins by NMR spectroscopy. *Prog. Retinal Eye Res.* **18**, 431–462
- Carver, J. A. and Lindner, R. A. (1998) NMR spectroscopy of α -crystallin. Insights into the structure, interactions and chaperone action of small heat-shock proteins. *Int. J. Biol. Macromol.* **22**, 197–209
- Carver, J. A., Aquilina, J. A., Truscott, R. J. W. and Ralston, G. B. (1992) Identification by ¹H NMR spectroscopy of flexible C-terminal extensions in bovine lens α -crystallin. *FEBS Lett.* **311**, 143–149
- Treweek, T. M., Ecroyd, H., Williams, D. M., Meehan, S., Carver, J. A. and Walker, M. J. (2007) Site-directed mutations in the C-terminal extension of human α B-crystallin affects chaperone function and blocks amyloid fibril formation. *PLoS ONE* **2**, e1046
- Bax, A. and Davis, D. G. (1985) MLEV-17-based two-dimensional homonuclear magnetization transfer spectroscopy. *J. Magn. Reson.* **65**, 355–360
- Kessler, H., Griesinger, C., Kerssebaum, R., Wagner, K. and Ernst, R. R. (1987) Separation of cross-relaxation and J cross-peaks in 2D rotating-frame NMR spectroscopy. *J. Am. Chem. Soc.* **109**, 607–609
- Reference deleted
- Zhang, L., Wang, H., Liu, D., Liddington, R. and Fu, H. (1997) Raf-1 kinase and exoenzyme S interact with 14-3-3 ζ through a common site involving lysine 49. *J. Biol. Chem.* **272**, 13717–13724
- Provencher, S. W. (1982) CONTIN: a general purpose constrained regularization program for inverting noisy linear algebraic and integral equations. *Comput. Phys. Commun.* **27**, 229–242
- Koppel, D. E. (1972) Analysis of macromolecular polydispersity in intensity correlation spectroscopy: the method of cumulants. *J. Chem. Phys.* **57**, 4814–4820
- Larkin, M. A., Blackshields, G., Brown, N. P., Chenna, R., McGettigan, P. A., McWilliam, H., Valentin, F., Wallace, I. M., Wilm, A., Lopez, R. et al. (2007) Clustal W and Clustal X version 2.0. *Bioinformatics* **23**, 2947–2948
- Romero, P., Obradovic, Z., Li, X., Garner, E. C., Brown, C. J. and Dunker, A. K. (2001) Sequence complexity of disordered protein. *Proteins* **42**, 38–48
- Li, X., Romero, P., Rani, M., Dunker, A. K. and Obradovic, Z. (1999) Predicting protein disorder for N-, C-, and internal regions. *Genome Inform. Ser. Workshop Genome Inform.* **10**, 30–40
- Romero, P., Obradovic, Z. and Dunker, K. (1997) Sequence data analysis for long disordered regions prediction in the calcineurin family. *Genome Inform. Ser. Workshop Genome Inform.* **8**, 110–124
- Prilusky, J., Felder, C. E., Zeev-Ben-Mordehai, T., Rydberg, E. H., Man, O., Beckmann, J. S., Silman, I. and Sussman, J. L. (2005) FoldIndex: a simple tool to predict whether a given protein sequence is intrinsically unfolded. *Bioinformatics* **21**, 3435–3438
- Wüthrich, K. (1986) *NMR of Proteins and Nucleic Acids*, Wiley, New York
- Wishart, D. S., Bigam, C. G., Holm, A., Hodges, R. S. and Sykes, B. D. (1995) ¹H, ¹³C and ¹⁵N random coil NMR chemical shifts of the common amino acids. I. Investigations of nearest-neighbor effects. *J. Biomol. NMR* **5**, 67–81
- Viscontii, S., Camoni, L., Marra, M. and Aducci, P. (2008) Role of the 14-3-3 C-terminal region in the interaction with the plasma membrane H⁺-ATPase. *Plant Cell Physiol.* **49**, 1887–1897
- Kumagai, I., Takeda, S. and Miura, K. (1992) Functional conversion of the homologous proteins α -lactalbumin and lysozyme by exon exchange. *Proc. Natl. Acad. Sci. U.S.A.* **89**, 5887–5891
- Masters, S. C. and Fu, H. (2001) 14-3-3 proteins mediate an essential anti-apoptotic signal. *J. Biol. Chem.* **276**, 45193–45200
- Wang, B., Yang, H., Liu, Y. C., Jelinek, T., Zhang, L., Ruoslahti, E. and Fu, H. (1999) Isolation of high-affinity peptide antagonists of 14-3-3 proteins by phage display. *Biochemistry* **38**, 12499–12504
- Treweek, T. M., Rekas, A., Walker, M. J. and Carver, J. A. (2010) A quantitative NMR spectroscopic examination of the flexibility of the C-terminal extensions of the molecular chaperones α A- and α B-crystallin. *Exp. Eye Res.* **91**, 691–699
- Treweek, T. M., Morris, A. M. and Carver, J. A. (2003) Intracellular protein unfolding and aggregation: the role of small heat-shock chaperone proteins. *Aust. J. Chem.* **56**, 357–367
- Esposito, G., Viglino, P., Fogolari, F., Gaestel, M. and Carver, J. A. (1998) Selective NMR experiments on macromolecules: implementation and analysis of QUIET-NOESY. *J. Magn. Reson.* **132**, 204–213
- Ecroyd, H. and Carver, J. A. (2008) The effect of small molecules in modulating the chaperone activity of α B-crystallin against ordered and disordered protein aggregation. *FEBS J.* **275**, 935–947
- Ecroyd, H., Meehan, S., Horwitz, J., Aquilina, J. A., Benesch, J. L., Robinson, C. V., Macphree, C. E. and Carver, J. A. (2007) Mimicking phosphorylation of α B-crystallin affects its chaperone activity. *Biochem. J.* **401**, 129–141
- Lindner, R. A., Carver, J. A., Ehrnsperger, M., Buchner, J., Esposito, G., Behlke, J., Lutsch, G., Kotlyarov, A. and Gaestel, M. (2000) Mouse Hsp25, a small shock protein. The role of its C-terminal extension in oligomerization and chaperone action. *Eur. J. Biochem.* **267**, 1923–1932
- Morris, A. M., Treweek, T. M., Aquilina, J. A., Carver, J. A. and Walker, M. J. (2008) Glutamic acid residues in the C-terminal extension of small heat shock protein 25 are critical for structural and functional integrity. *FEBS J.* **275**, 5885–5898
- Smulders, R. H. P. H., Carver, J. A., Lindner, R. A., Van Boekel, M. A., Bloemendal, H. and De Jong, W. W. (1996) Immobilization of the C-terminal extension of bovine α A-crystallin reduces chaperone-like activity. *J. Biol. Chem.* **271**, 29060–29066
- Vicart, P., Caron, A., Guicheney, P., Li, Z., Prevost, M. C., Faure, A., Chateau, D., Chapon, F., Tome, F., Dupret, J. M. et al. (1998) A missense mutation in the α B-crystallin chaperone gene causes a desmin-related myopathy. *Nat. Genet.* **20**, 92–95
- Treweek, T. M., Rekas, A., Lindner, R. A., Walker, M. J., Aquilina, J. A., Robinson, C. V., Horwitz, J., Perng, M. D., Quinlan, R. A. and Carver, J. A. (2005) R120G α B-crystallin promotes the unfolding of reduced α -lactalbumin and is inherently unstable. *FEBS J.* **272**, 711–724

- 47 Bova, M. P., Yaron, O., Huang, Q., Ding, L., Haley, D. A., Stewart, P. L. and Horwitz, J. (1999) Mutation R120G in α B-crystallin, which is linked to a desmin-related myopathy, results in an irregular structure and defective chaperone-like function. *Proc. Natl. Acad. Sci. U.S.A.* **96**, 6137–6142
- 48 Bova, M. P., Ding, L.-L., Horwitz, J. and Fung, B. K.-K. (1997) Subunit exchange of α A-crystallin. *J. Biol. Chem.* **272**, 29511–29517
- 49 Laganowsky, A., Benesch, J. L., Landau, M., Ding, L., Sawaya, M. R., Cascio, D., Huang, Q., Robinson, C. V., Horwitz, J. and Eisenberg, D. (2010) Crystal structures of truncated α A and α B crystallins reveal structural mechanisms of polydispersity important for eye lens function. *Protein Sci.* **19**, 1031–1043
- 50 Carver, J. A., Lindner, R. A., Lyon, C., Canet, D., Hernandez, H., Dobson, C. M. and Redfield, C. (2002) The interaction of the molecular chaperone α -crystallin with unfolding α -lactalbumin: a structural and kinetic spectroscopic study. *J. Mol. Biol.* **318**, 815–827
- 51 Carver, J. A., Rekas, A., Thorn, D. C. and Wilson, M. R. (2003) Small heat-shock proteins and clusterin: intra- and extracellular molecular chaperones with a common mechanism of action and function? *IUBMB Life* **55**, 661–668
- 52 Lindner, R. A., Kapur, A., Mariani, M., Titmuss, S. J. and Carver, J. A. (1998) Structural alterations of α -crystallin during its chaperone action. *Eur. J. Biochem.* **258**, 170–183
- 53 Ecroyd, H. and Carver, J. A. (2009) Crystallin proteins and amyloid fibrils. *Cell. Mol. Life Sci.* **66**, 62–81
- 54 Sadik, G., Tanaka, T., Kato, K., Yamamori, H., Nessa, B. N., Morihara, T. and Takeda, M. (2009) Phosphorylation of tau at Ser²¹⁴ mediates its interaction with 14-3-3 protein: implications for the mechanism of tau aggregation. *J. Neurochem.* **108**, 33–43
- 55 Hernandez, F., Cuadros, R. and Avila, J. (2004) 14-3-3 ζ protein favours the formation of human tau fibrillar polymers. *Neurosci. Lett.* **357**, 143–146
- 56 Chen, H.-K., Fernandez-Funez, P., Acevedo, S. F., Lam, Y. C., Kaytor, M. D., Fernandez, M. H., Aitken, A., Skoulakis, E. M. C., Orr, H. T., Botas, J. and Zoghbi, H. Y. (2003) Interaction of Akt-phosphorylated ataxin-1 with 14-3-3 mediates neurodegeneration in spinocerebellar ataxia type-1. *Cell* **113**, 457–468
- 57 Petosa, C., Masters, S. C., Bankston, L. A., Pohl, J., Wang, B., Fu, H. and Liddington, R. C. (1998) 14-3-3 ζ binds a phosphorylated Raf peptide and an unphosphorylated peptide via its conserved amphipathic groove. *J. Biol. Chem.* **273**, 16305–16310

Received 4 January 2011/19 April 2011; accepted 10 May 2011

Published as BJ Immediate Publication 10 May 2011, doi:10.1042/BJ20102178